an extremely thin (~3 nm) facet. In particular, the nearly perfect fluorescence quenching of its NT_2 block substantiates that electronic effects of heterojunctions can indeed propagate over a micrometer-long distance through a great number of π-stacks in semiconducting organic materials.

References and Notes

1. M. T. Björk *et al.*, *Nano Lett.* **2**, 87 (2002).
2. S. Banerjee, S. S. Wong, *Nano Lett.* **2**, 195 (2002).
3. O. Harnack, C. Pacholski, H. Weller, A. Yasuda, J. M. Wessels, *Nano Lett.* **3**, 1097 (2003).
4. B. Tian *et al.*, *Nature* **449**, 885 (2007).
5. A. I. Hochbaum, P. Yang, *Chem. Rev.* **110**, 527 (2010).
6. F.-S. Tsai *et al.*, *Appl. Phys. Express* **4**, 025002 (2011).
7. S. Günes, H. Neugebauer, N. S. Sariciftci, *Chem. Rev.* **107**, 1324 (2007).
8. B. C. Thompson, J. M. J. Fréchet, *Angew. Chem. Int. Ed.* **47**, 58 (2008).
9. G. Yu, J. Gao, J. C. Hummelen, F. Wudl, A. J. Heeger, *Science* **270**, 1789 (1995).
10. P. Peumans, S. Uchida, S. R. Forrest, *Nature* **425**, 158 (2003).
11. G. Li *et al.*, *Nat. Mater.* **4**, 864 (2005).
12. J. Y. Kim *et al.*, *Science* **317**, 222 (2007).
13. T. F. A. De Greef *et al.*, *Chem. Rev.* **109**, 5687 (2009).
14. F. J. M. Hoeben, P. Jonkheijm, E. W. Meijer, A. P. H. J. Schenning, *Chem. Rev.* **105**, 1491 (2005).
15. F. Würthner *et al.*, *J. Am. Chem. Soc.* **126**, 10611 (2004).
16. Y. Yamamoto *et al.*, *Science* **314**, 1761 (2006).
17. A. L. Sisson *et al.*, *Angew. Chem. Int. Ed.* **47**, 3727 (2008).
18. Y. Yamamoto *et al.*, *Proc. Natl. Acad. Sci. U.S.A.* **106**, 21051 (2009).
19. N. Sakai, R. Bhosale, D. Emery, J. Mareda, S. Matile, *J. Am. Chem. Soc.* **132**, 6923 (2010).
20. By using crystallizable core units, the formation of rodlike block co-micelles has been demonstrated (*21–24*).
21. X. Wang *et al.*, *Science* **317**, 644 (2007).
22. T. Gädt, N. S. Ieong, G. Cambridge, M. A. Winnik, I. Manners, *Nat. Mater.* **8**, 144 (2009).
23. J. B. Gilroy *et al.*, *Nat. Chem.* **2**, 566 (2010).
24. S. K. Patra *et al.*, *J. Am. Chem. Soc.* **133**, 8842 (2011).
25. J. P. Hill *et al.*, *Science* **304**, 1481 (2004).
26. W. Jin *et al.*, *J. Am. Chem. Soc.* **130**, 9434 (2008).
27. Materials and methods are available as supporting material on *Science* Online.
28. W. Zhang, W. Jin, T. Fukushima, N. Ishii, T. Aida, *Angew. Chem. Int. Ed.* **48**, 4747 (2009).
29. G. Zhang *et al.*, *J. Am. Chem. Soc.* **129**, 719 (2007).
30. A. Saeki, T. Fukumatsu, S. Seki, *Macromolecules* **44**, 3416 (2011).

Acknowledgments: We thank E. Ohta (RIKEN) for DFT calculation of HBC **2**. W.Z. thanks the Japan Society for the Promotion of Science Young Scientist Fellowship (21•9925). T.F. thanks Ministry of Education, Culture, Sports, Science, and Technology, Japan, for financial support (21350108).

Supporting Online Material

www.sciencemag.org/cgi/content/full/334/6054/340/DC1
Materials and Methods
Figs. S1 to S11
References (*31–33*)

27 June 2011; accepted 14 September 2011
10.1126/science.1210369

Dynamics of the Reaction of Methane with Chlorine Atom on an Accurate Potential Energy Surface

Gábor Czakó* and Joel M. Bowman

The reaction of the chlorine atom with methane has been the focus of numerous studies that aim to test, extend, and/or modify our understanding of mode-selective reactivity in polyatomic systems. To this point, theory has largely been unable to provide accurate results in comparison with experiments. Here, we report an accurate global potential energy surface for this reaction. Quasi-classical trajectory calculations using this surface achieve excellent agreement with experiment on the rotational distributions of the hydrogen chloride (HCl) product. For the $Cl + CHD_3 \rightarrow HCl + CD_3$ reaction at low collision energies, we confirm the unexpected experimental finding that CH-stretch excitation is no more effective in activating this late-barrier reaction than is the translational energy, which is in contradiction to expectations based on results for many atom-diatom reactions.

Decades of experimental and theoretical studies of atom-diatom reactions led to a well-validated framework for predicting the effect of vibrational excitation on the ensuing dynamics (*1*, *2*). Earlier fundamental research demonstrated the importance of the reaction barrier location on the efficacy of partitioning the total energy between internal excitation of the diatomic molecule and relative translational energy of the reactants. The careful and correct analysis of these reactions led to the "Polanyi rules" (*3*), which state that vibrational energy is more efficient than is translational energy in activating a late-barrier reaction, whereas the reverse is true for an early-barrier reaction. Recent studies have investigated the generality and validity of these paradigms for polyatomic systems. The X + methane (CH_4 and deuterated isotopologues) reactions (which replace the diatomic with a five-atom molecule) have played a central role in this research, in which, for example, the choice of X as H, O, F, and Cl has permitted the height and location of the reaction barrier to vary widely. Recent experiments by Liu and co-workers (*4–8*) on the F and Cl + methane reactions have uncovered surprising departures from expectations that present a strong challenge to theory, which ultimately provides detailed understanding of chemical reaction dynamics. A rigorous theoretical approach to reaction analysis consists of two components. The first is to determine the global potential energy surface (PES) (*9*), which governs the nuclear motion, and the second is to perform dynamics calculations with the PES. We succeeded in carrying out this process recently for the early-low-barrier $F + CHD_3$ reaction, for which we were able to illuminate the surprising experimental result of the enhancement of the $DF + CHD_2$ channel by exciting the CH-stretch (*10*, *11*). In this Report, we take the same approach to address and interpret experiments on the late-high-barrier $Cl + CHD_3$ reaction by Liu and co-workers (*5*), which also uncovered a surprising result, namely that at low collision energies (E_{coll}) vibrational excitation of the CH-stretch was no more effective than was translational energy in promoting the reaction. This result, as pointed out by these authors, contradicts the rule of thumb of reaction dynamics (Polanyi rules). Other interesting experimental results of this reaction are also successfully addressed.

As with the previous accurate PES for $F + CH_4$ (*10*), the $Cl + CH_4$ PES is a permutationally invariant fit (*12*, *9*) to roughly 16,000 high-level ab initio electronic energies. The selection of configurations for the PES is quite similar to procedures used for the $F + CH_4$ PES (*10*, *12*), and details are given in (*13*). A key part of this approach is the use of an electronic structure method that gives accurate energies, especially for the barrier height, reaction enthalpy, and the entrance and exit channel van der Waals (vdW) wells. These wells, which result from long-range attractive interactions, are ubiquitous in chemistry, and as we show here, the prereactive one has a substantial effect on the $Cl + CHD_3$ reaction dynamics at low collision energies. The inclusion of the spin-orbit (SO) correction is also essential in the present case because it effectively increases the barrier height and reaction endoergicity by 0.8 kcal/mol and has a substantial effect on the entrance channel vdW well. (The SO correction is a relativistic effect, which lowers the energy of the halogen atoms and has about twice as large an energy shift on the heavier Cl than on F. The widely applied nonrelativistic electronic structure computations neglect this effect.) There is also a substantial basis set–superposition error in this region, which has to be corrected. Thus, the goal for the present PES is to take all of this into account. In order to achieve this goal, we used a composite electronic structure method, which provides accurate energies with affordable computational time. The general composite approach (*14*), which is widely used, combines results from several levels of ab initio method and basis (*15*, *16*). Second, in order to account for the SO effect differences between the SO and non-SO ground-state electronic energies, obtained by means of multireference configuration interaction (MRCI) with Davidson correction (MRCI + Q) with basis set aug-cc-pVTZ (MRCI + Q/aug-cc-pVTZ), were added to

Cherry L. Emerson Center for Scientific Computation and Department of Chemistry, Emory University, Atlanta, GA 30322, USA.

*To whom correspondence should be addressed. E-mail: czako@chem.elte.hu

the composite non-SO energies at 1598 $ClCH_4$ configurations in the entrance channel, where the SO corrections are substantial and nonconstant. (2000 Cl + CH_4 fragment data were also shifted by the constant SO correction of the Cl atom.) Third, counterpoise correction for entrance channel basis set–superposition error at the above-mentioned 1598 configurations was applied. The present PES is based on electronic energies with basis set effects up to aug-cc-pCVTZ (correlation-consistent polarized core-valence triple-zeta basis augmented with diffuse functions) (*17*); electron correlation up to the "gold standard" CCSD(T) (coupled-cluster with single and double and perturbative triple excitations) method (*18*); correlation effects of the core-core and core-valence electrons; and SO and counterpoise corrections for the entrance channel. As a result, this present PES corresponds to the SO ground state, accurately describes the vdW regions both in the entrance and exit channels, and describes both the abstraction (HCl + CH_3) and substitution (H + CH_3Cl) channels. Thus, it represents a considerable advance over previous PESs for Cl + CH_4, including several semiempirical (*19*, *20*) and ab initio–based surfaces in 2 (*21*), 3 (*22*), and 12(full) (*23*) dimensions.

A schematic of the PES, given in Fig. 1, shows the stationary-point structures and energies of the abstraction and substitution reactions $Cl(^2P_{3/2}, {}^2P) + CH_4 \rightarrow HCl + CH_3$ and H + CH_3Cl, where $Cl(^2P_{3/2})$ is the SO ground state of the Cl atom lying below the non-SO energy of $Cl(^2P)$ by 0.8 kcal/mol. The vdW wells in the entrance channel for the CH–Cl and HC–Cl linear bond arrangements are below $Cl(^2P_{3/2}) + CH_4$(eq) by 0.3 and 0.6 kcal/mol, respectively. (That the most favorable vdW orientation is the HC–Cl one is both meaningful and easily understood from a simple sum-of-pairs interaction because C is more polarizable than H.) The abstraction reaction has a late (product-like) saddle-point of energy 7.6 kcal/mol relative to $Cl(^2P_{3/2}) + CH_4$(eq) and a vdW well in the product channel with a dissociation energy (D_e) of 2.4 kcal/mol. The PES reaction endoergicity for the HCl + CH_3 channel is 5.7 kcal/mol. These values are in excellent agreement with our benchmark energies of 7.6, 2.4, and 6.0 kcal/mol, respectively, which were obtained by using the focal-point analysis (FPA) approach (*14*) [see computational details in (*24*)]. The PES reaction endoergicity is also in excellent agreement with the experimental value, deduced to be 6.0 kcal/mol (*13*).

None of the previous PESs are as accurate in all of these key energies. In particular, focusing on the important entrance and exit channel vdW wells, the present PES contains an accurate description of the latter, (CH_3—HCl), with a substantial D_e value of 2.4 kcal/mol. This contrasts with the conclusion based on a semiempirical PES with a D_e of 0.3 kcal/mol that "the existence of this product complex is questionable" (*20*). With respect to the entrance channel vdW well, there are even greater contrasts with previous PESs. This vdW region in particular is affected by SO

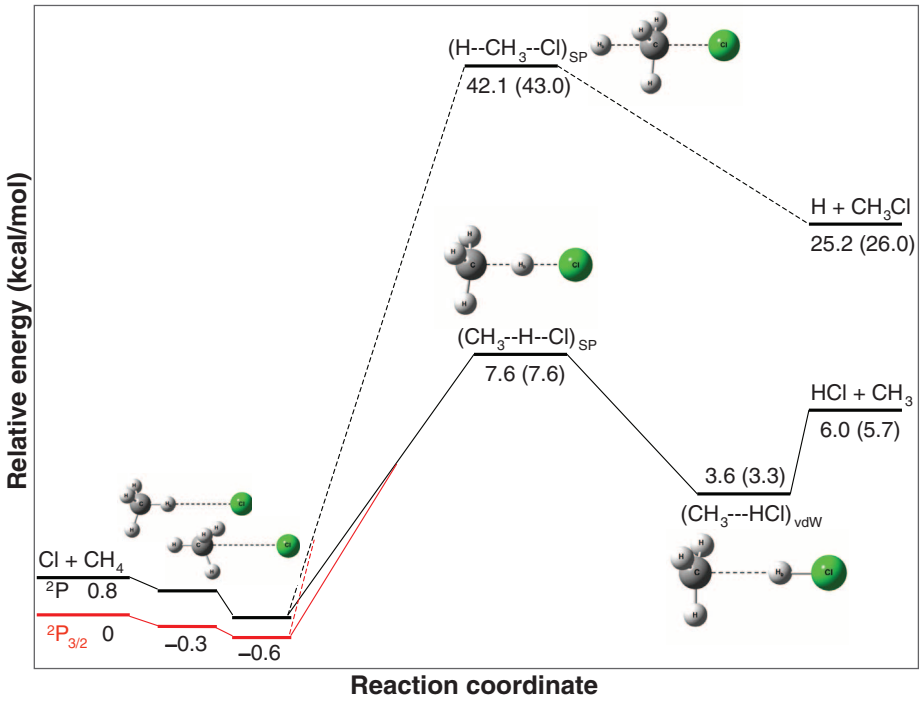

Fig. 1. Schematic of the global SO and non-SO ground-state PESs of the Cl + CH_4 reaction showing the accurate benchmark energies and the PES values in parentheses; for example, 7.6 (7.6) shows the excellent agreement between the benchmark and PES barrier heights. All the energies are relative to the SO ground state $Cl(^2P_{3/2})$ + CH_4(eq). The negative energies correspond to the attractive region of the vdW well in the entrance channel on the SO surface (Fig. 2).

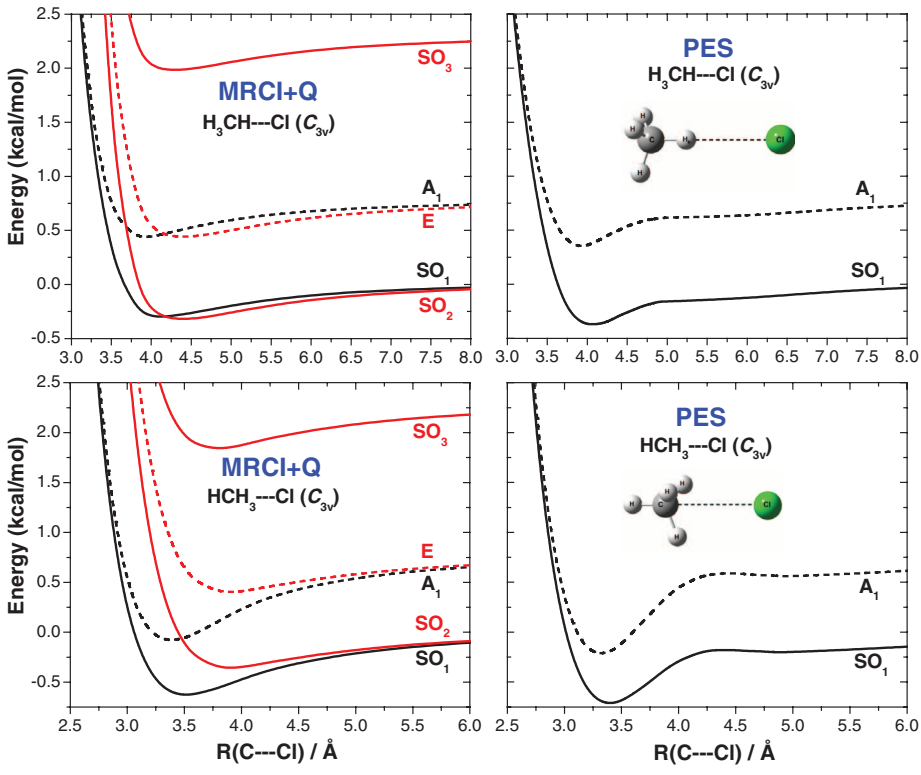

Fig. 2. Potential energy curves of CH_4–Cl as a function of the C–Cl distance along the C_{3v} axis with fixed CH_4(eq) geometry and (**top**) CH–Cl or (**bottom**) HC–Cl linear bond arrangements that were (**left**) computed at the MRCI+Q/aug-cc-pVTZ level or (**right**) obtained from the non-SO– and SO-corrected ground-state PESs. A_1 and E denote the ground and excited non-SO electronic states, respectively, and SO_1, SO_2, SO_3 are the three SO states. The energies are relative to $Cl(^2P_{3/2})$ + CH_4(eq).

interaction, as shown in Fig. 2, where potential curves both with and without SO coupling are shown for the entrance channel. Our multireference configuration interaction results show that the non-SO electronic ground state potential has minima with CH–Cl and HC–Cl bond arrangements with depths of 0.3 kcal/mol and 0.9 kcal/mol, respectively (*25*). The SO interaction has a minor effect on the former, whereas it decreases the depth of the latter by 0.3 kcal/mol; but, the HC–Cl orientation still remains the deeper minimum. It is critical that the present PES describes these vdW regions accurately, as shown in Fig. 2, because they play an important role in the low E_{coll} dynamics. [Additional comparisons between the PES and benchmark properties, including data for the substitution channel, are presented in (*13*).]

Having shown the high accuracy of the PES by comparison with benchmark ab initio data, we applied it to simulations of the collision dynamics of the title reaction. We performed more than 2 million quasi-classical trajectories (QCTs) for the reactions of $Cl(^2P_{3/2})$ with $CH_4(v=0)$, $CHD_3(v=0)$, and $CHD_3(v_k=1)$ [$k=1, 3, 6, 5$], where $v=0$, $v_1=1$, and $v_k=1$ [$k=3, 6, 5$] denote the vibrational ground state, CH-stretch, and three different bend excitations, respectively. Details of the QCT calculations are given in (*13*). Classical zero-point leak and vibrational energy relaxation from $v_k=1$ was investigated thoroughly for CHD_3 and found not to be a serious issue, as already reported in (*8*, *11*) and discussed further in (*13*). All the results presented below correspond to the SO-corrected PES. Computations on the non-SO PES show that the inclusion of the SO correction in the PES decreases the cross sections by

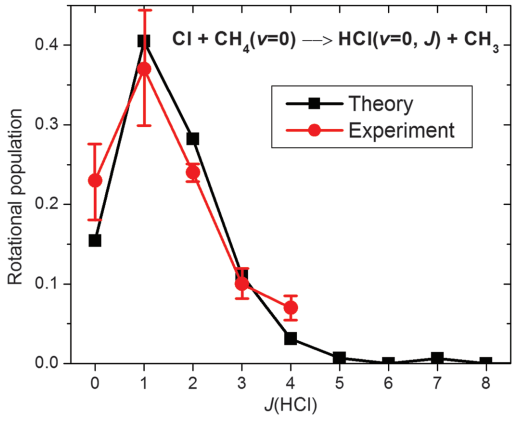

Fig. 3. Computed and experimental HCl rotational distributions for the Cl + CH_4 reaction at a collision energy of 3.7 kcal/mol. Theory uses quasi-classical trajectory calculations on the SO-corrected PES considering trajectories in which CH_3 has at least zero-point vibrational energy. Experimental data are taken from (*28*). On the basis of analysis of two batches of trajectories, the estimated statistical uncertainty of the computed results is less than 15%.

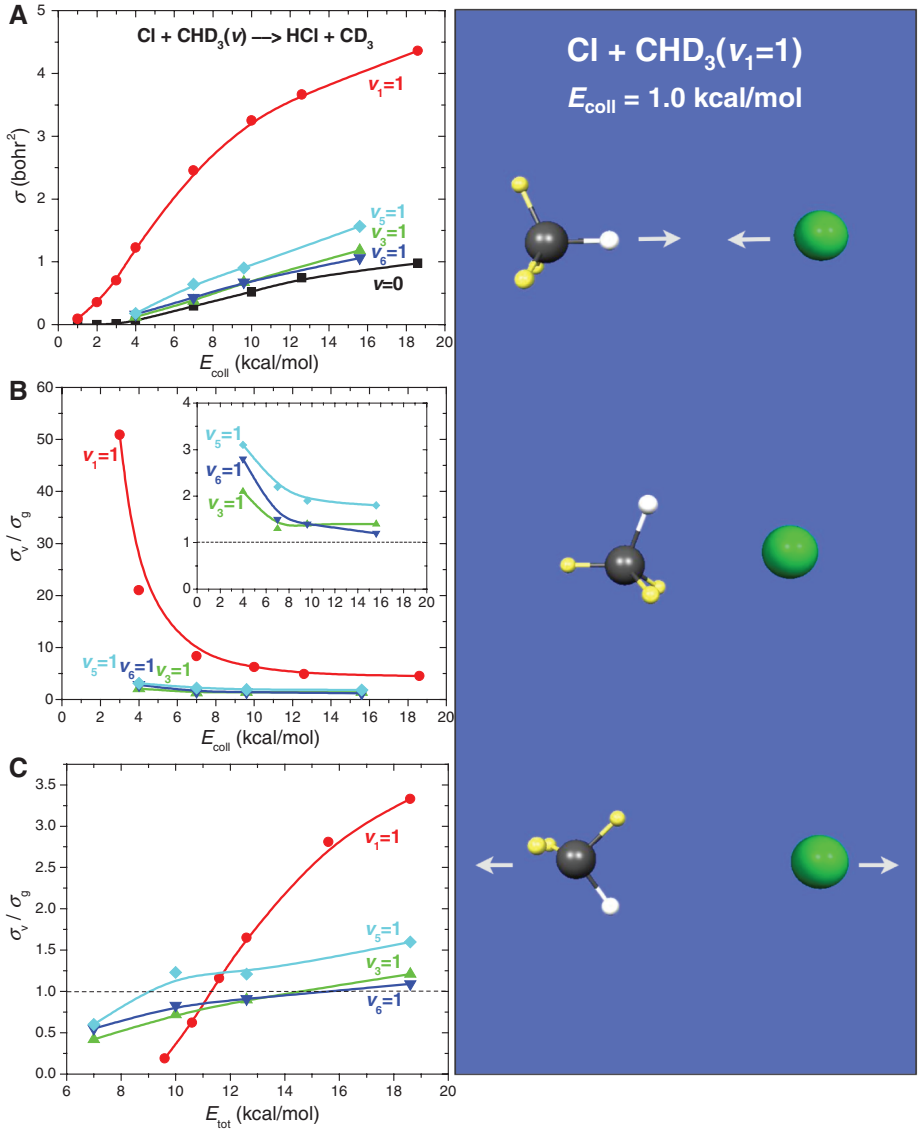

Fig. 4. (**A**) Computed cross sections for the ground state ($v=0$) and reactant CH-stretch ($v_1=1$) and bend ($v_k=1$) [$k=3, 6, 5$] excited Cl + $CHD_3(v) \rightarrow$ HCl + CD_3 reactions and (**B**) their ratios as a function of E_{coll}. (**C**) Cross section ratios at equivalent amount of total energy ($E_{tot} = E_{coll} + E_v$), where the vibrational energies (E_v) are 0, 8.6, and 3.0 kcal/mol (relative to zero-point energy) for the ground state and stretch- and bend-excited reactions, respectively. (Right) Snapshots of a nonreactive Cl + $CHD_3(v_1=1)$ trajectory illustrating the stereodynamics in the vdW region causing the unexpected $\sigma_v/\sigma_g < 1$ ratio at $E_{tot} = 9.6$ kcal/mol, as seen in (C).

a factor of 1.5 to 2.5 at low E_{coll} because of the increase in the barrier height, but it has no substantial effect on the final state distributions.

First, consider the HCl(v = 0, J) rotational distributions for the Cl + CH_4(v = 0) reaction. These were reported by three experimental groups showing extremely cold rotational populations (*26*–*28*). Theoretical simulations have been struggling to reproduce this rotational distribution for many years; the previous work overestimates the rotational temperature of the HCl product ensemble (*19*, *23*, *29*). In Fig. 3, we present QCT results obtained by using the present PES and, as seen, the agreement between theory and experiment (*27*, *28*) is excellent. We also computed the HCl rotational distributions for Cl + CHD_3(v_1 = 1) showing cold rotational distribution of the stretch-excited product HCl(v = 1, J), similar to HCl(v = 0, J) from Cl + CH_4(v = 0), and substantially hotter rotational temperature of the vibrationally ground state HCl in qualitative agreement with an older experiment (which had large uncertainties) (*30*).

Next, we considered the effect of vibrational excitation in CHD_3, mentioned already. The Polanyi rules (*3*) state that for late-barrier (atom + diatom) reactions, the reactant vibrational energy is more efficient than is the translational energy in surmounting the barrier. However, as noted already a recent crossed molecular beam experiment (*5*) found that this picture could not be simply extended for the Cl + CHD_3 reaction. To investigate this finding, we calculated cross sections for the reactant ground state and bend and CH-stretch–excited Cl + CHD_3(v_k) → HCl + CD_3 reactions and show the results in Fig. 4 as a function of both E_{coll} and total energy (E_{tot}). At the same value of E_{coll}, we see that all the bending and especially the CH-stretch excitations enhance the reaction relative to Cl + CHD_3(v = 0) (Fig. 4, A and B). Thus, in this sense there is enhancement of the reaction by excitation of these modes. However, as noted in the experimental study, at the same E_{tot} translational energy is more effective than the excitation of the reactive CH-stretch or bend at low E_{coll}. As the E_{coll} increases, the intuitively expected enhancement of reactivity is seen upon vibrational excitation. This is best seen by plotting cross section ratios (σ_v/σ_g) as a function of E_{tot} (Fig. 4C). As seen, σ_v/σ_g is less than 1 if the E_{tot} is below 11 and (15, 15, 9) kcal/mol for the CH-stretch and (v_3, v_6, v_5) bending modes, respectively. Only CD_3(v = 0) products were probed experimentally, whereas theory shows the total reactivity. Correlating the QCT cross sections to CD_3(v = 0) results in a decrease of the $\sigma_{CH}/\sigma_{ground}$ ratio, improving the agreement with the measured data (fig. S1). Furthermore, the experiment applied thermal bending excitation; thus, the measured bending cross sections show the average effect of the three bending modes (*5*). Theory predicts that the $v_5(e)$ (CD_3 deformation) bending mode is the most efficient to drive the reaction (Fig. 4B), similar to F + CHD_3. Overall, both theory and experiment show that the same amount of total energy distributed among different nuclear motions has different effects on chemical reactivity.

In order to gain insight into these results, we examined the trajectories for the ground and stretch-excited CHD_3 at the same E_{tot} of 9.6 kcal/mol, thus corresponding to a low E_{coll} for CHD_3(v_1 = 1). We determined the distributions of the smallest H-Cl and C-Cl distances for nonreactive trajectories and, as shown in fig. S2, most of the trajectories for the CH-stretch–excited reaction do not reach the transition state. Instead, the Cl atom turns back at the vdW region in the $r_{C\text{-}Cl}$ = 2.9 to 3.5 Å range. This occurs because at low E_{coll}, the CHD_3 rotates to the energetically favorable, but nonreactive, H-C–Cl orientation (Fig. 4, right). Thus, at low E_{coll} the entrance channel vdW well orients the reactants in an unreactive configuration. At higher collision energies, this effect is diminished, and the expected enhancement of the reaction for the stretch-excited CHD_3 (over translational energy) is seen.

Next, we considered the experimental results on the vibrational distribution of HCl (*5*). As noted in (*5*), vibrationally adiabatic theory predicts that the ground state and CH-stretch–excited Cl + CHD_3 reactions produce exclusively HCl(v = 0) and HCl(v = 1) products, respectively. Experiment found the breakdown of this simple theory for the excited reaction because the measured fraction of HCl(v = 1), correlated to CD_3(v = 0), was only 45% (*5*). Our dynamics calculations show that at higher E_{coll}, above the energetic threshold for HCl(v = 1), the ground-state reaction still produces mainly HCl(v = 0), and the fraction of HCl(v = 1) is only 1% with only a slight E_{coll} dependence. This small ratio increases to about 2% if the results are correlated to CD_3(v = 0), which is in quantitative agreement with experiment (*5*). The reactant CH-stretch excitation increases the fraction of HCl(v = 1) to 10% and 30 to 50% for all the CD_3 states and CD_3(v = 0), respectively, which is again in good agreement with the above-mentioned correlated experiment (*5*). The computations support the experimental observation: The ground state reaction is vibrationally adiabatic, whereas the CH-stretch excited reaction is nonadiabatic.

Last to be considered was the very recent experiment (*6*) on steric control of Cl + CHD_3(v_1 = 1). We have performed QCT calculations with aligned CHD_3(v_1 = 1) in which the CH-stretch is parallel or perpendicular to the initial relative velocity vector of the reactants. We found that the total reactivity of H-abstraction is higher at parallel alignment relative to that at perpendicular orientations, which is in agreement with experiment (*6*). The trajectories show that the initial orientation is maintained while the Cl approaches CHD_3(v_1 = 1), supporting the recent experiment (*6*). However, at the turning point the QCTs show substantial energy transfer causing rotational excitation of CHD_3, and the prealignment is not conserved after the collision (Fig. 4, right).

References and Notes

1. L. Che *et al.*, *Science* **317**, 1061 (2007).
2. D. Skouteris *et al.*, *Science* **286**, 1713 (1999).
3. J. C. Polanyi, *Science* **236**, 680 (1987).
4. J. J. Lin, J. Zhou, W. Shiu, K. Liu, *Science* **300**, 966 (2003).
5. S. Yan, Y.-T. Wu, B. Zhang, X.-F. Yue, K. Liu, *Science* **316**, 1723 (2007).
6. F. Wang, J.-S. Lin, K. Liu, *Science* **331**, 900 (2011).
7. W. Zhang, H. Kawamata, K. Liu, *Science* **325**, 303 (2009).
8. G. Czakó, Q. Shuai, K. Liu, J. M. Bowman, *J. Chem. Phys.* **133**, 131101 (2010).
9. J. M. Bowman, G. Czakó, B. Fu, *Phys. Chem. Chem. Phys.* **13**, 8094 (2011).
10. G. Czakó, B. C. Shepler, B. J. Braams, J. M. Bowman, *J. Chem. Phys.* **130**, 084301 (2009).
11. G. Czakó, J. M. Bowman, *J. Am. Chem. Soc.* **131**, 17534 (2009).
12. B. J. Braams, J. M. Bowman, *Int. Rev. Phys. Chem.* **28**, 577 (2009).
13. Materials and methods are available as supporting material on *Science* Online.
14. A. G. Császár, W. D. Allen, H. F. Schaefer, *J. Chem. Phys.* **108**, 9751 (1998).
15. The composite energies were obtained as E[UCCSD(T)/aug-cc-pVDZ] + E[AE-UMP2/aug-cc-pCVTZ] − E[UMP2/aug-cc-pVDZ], where AE denotes correlating all the electrons. For the entrance channel, counterpoise and spin-orbit corrections were computed at the AE-UMP2/aug-cc-pCVTZ and MRCI+Q/aug-cc-pVTZ levels of theory, respectively. The PES was represented by a polynomial expansion in y_{ij} = exp(−r_{ij}/a) (where a = 2 bohr), including all terms up to total degree six. 3262 coefficients were determined by a weighted linear least-squares fit of roughly 16,000 energy points. The root mean square (RMS)–fitting errors are 0.2, 0.4, and 1.0 kcal/mol for energy intervals (0, 31), (31, 63), and (63, 143), respectively.
16. For 15 arbitrary geometries with energies in the wide 0 to 36 kcal/mol range, we found that this composite method gives results comparable with extremely high-quality all-electron CCSD(T)/aug-cc-pCVQZ calculations with a RMS of only 0.4 kcal/mol, whereas the RMS error of high-level CCSD(T)/aug-cc-pVTZ calculations is 1.1 kcal/mol. Furthermore, the composite method reduces the computational time by factors of about 1000 and 5 relative to the above-mentioned high-level computations, respectively.
17. K. A. Peterson, T. H. Dunning Jr., *J. Chem. Phys.* **117**, 10548 (2002).
18. K. Raghavachari, G. W. Trucks, J. A. Pople, M. Head-Gordon, *Chem. Phys. Lett.* **157**, 479 (1989).
19. J. C. Corchado, D. G. Truhlar, J. Espinosa-García, *J. Chem. Phys.* **112**, 9375 (2000).
20. C. Rangel, M. Navarrete, J. C. Corchado, J. Espinosa-García, *J. Chem. Phys.* **124**, 124306 (2006).
21. S. T. Banks, D. C. Clary, *Phys. Chem. Chem. Phys.* **9**, 933 (2007).
22. H.-G. Yu, G. Nyman, *J. Chem. Phys.* **111**, 6693 (1999).
23. J. F. Castillo, F. J. Aoiz, L. Bañares, *J. Chem. Phys.* **125**, 124316 (2006).
24. The benchmark FPA study considers extrapolation to the complete basis set limit using aug-cc-pVnZ [n = 5 and 6] bases, electron correlation beyond CCSD(T), core correlation effects, scalar relativistic effects, and spin-orbit corrections.
25. These relative energies are benchmarked at the highly accurate CCSD(T)/aug-cc-pCVQZ level of theory correlating all the electrons, including corrections for the basis set superposition error.
26. W. R. Simpson, T. P. Rakitzis, S. A. Kandel, T. Lev-On, R. N. Zare, *J. Phys. Chem.* **100**, 7938 (1996).
27. D. F. Varley, P. J. Dagdigian, *J. Phys. Chem.* **99**, 9843 (1995).
28. C. Murray, B. Retail, A. J. Orr-Ewing, *Chem. Phys.* **301**, 239 (2004).
29. S. J. Greaves *et al.*, *Phys. Chem. Chem. Phys.* **13**, 11438 (2011).
30. W. R. Simpson, T. P. Rakitzis, S. A. Kandel, A. J. Orr-Ewing, R. N. Zare, *J. Chem. Phys.* **103**, 7313 (1995).

Acknowledgments: G.C. thanks the National Science Foundation (grant CHE-0625237), and J.M.B. thanks the U.S. Department of Energy (grant DE-FG02-97ER14782) for financial support.

Supporting Online Material

www.sciencemag.org/cgi/content/full/334/6054/343/DC1
Materials and Methods
Figs. S1 to S3
Tables S1 to S3

17 May 2011; accepted 9 September 2011
10.1126/science.1208514